

Conformational Similarities in the β -Ionone Ring Region of the Rhodopsin Chromophore in Its Ground State and after Photoactivation to the Metarhodopsin-I Intermediate[†]

Paul J. R. Spooner,^{*,‡,§} Jonathan M. Sharples,^{‡,§} Scott C. Goodall,[‡] Henning Seedorf,^{‡,‡} Michiel A. Verhoeven,[§] Johan Lugtenburg,[§] Petra H. M. Bovee-Geurts,^{||} Willem J. DeGrip,^{||,§} and Anthony Watts^{*,‡}

The Biomembrane Structure Unit, Department of Biochemistry, University of Oxford, South Parks Road, Oxford OX1 3QU, U.K., Leiden Institute of Chemistry, Gorlaeus Laboratories, Einsteinweg 55, 2333 CC Leiden, The Netherlands, and Nijmegen Center for Molecular Life Sciences, Department of Biochemistry, UMC-160, University of Nijmegen Medical School, 6500 HB Nijmegen, The Netherlands

Received August 6, 2003; Revised Manuscript Received October 10, 2003

ABSTRACT: High-resolution solid-state NMR methods have been used to analyze the conformation of the chromophore in the late photointermediate metarhodopsin-I, from observation of ¹³C nuclei introduced into the β -ionone ring (at the C16, C17, and C18 methyl groups) and into the adjoining segment of the polyene chain (at C8). Bovine rhodopsin in its native membrane was also regenerated with retinal that was ¹³C-labeled close to the 11-Z bond (C20 methyl group) to provide a reporter for optimizing and quantifying the photoconversion to metarhodopsin-I. Indirect photoconversion via the primary intermediate, bathorhodopsin, was adopted as the preferred method since ~44% conversion to the metarhodopsin-I component could be achieved, with only low levels (~18%) of ground-state rhodopsin remaining. The additional photoproduct, isorhodopsin, was resolved in ¹³C spectra from C8 in the chain, at levels of ~38%, and was shown using rotational resonance NMR to adopt the 6-s-cis conformation between the ring and the polyene chain. The C8 resonance was not shifted in the metarhodopsin-I spectral component but was strongly broadened, revealing that the local conformation had become less well defined in this segment of the chain. This line broadening slowed rotational resonance exchange with the C17 and C18 ring methyl groups but was accounted for to show that, despite the chain being more relaxed in metarhodopsin-I, its average conformation with respect to the ring was similar to that in the ground state protein. Conformational restraints are also retained for the C16 and C17 methyl groups on photoactivation, which, together with the largely preserved conformation in the chain, argues convincingly that the ring remains with strong contacts in its binding pocket prior to activation of the receptor. Previous conclusions based on photocrosslinking studies are considered in view of the current findings.

The visual pigment rhodopsin has long been considered a paradigm for the pharmacologically important superfamily of G protein-coupled receptors (GPCRs).¹ This presumed role

has become strengthened since the publication of the 3D crystallographic structure of bovine rhodopsin (1, 2), the first high-resolution structure for a GPCR. This structure now forms the basis for making homology predictions for related GPCRs (3–5) and for designing experiments to help understand how photoactivation of the chromophore in rhodopsin leads to the active state of the receptor which binds the specific G protein, transducin, and so catalyzes the sequence of biochemical events that result in the neural response.

Following photoisomerization of the 11-Z-retinylidene chromophore to the 11-E (all-trans) configuration, the protein proceeds through a number of short-lived (ns to μ s) intermediates to the first long-lived (ms) state, metarhodopsin-I (6). Metarhodopsin-I itself does not activate transducin, but is in a pH- and temperature-dependent equilibrium with the active state of the protein, metarhodopsin-II (6). Since at neutral pH the apoprotein, opsin, possesses negligible

[†] BBSRC are thanked for financial support (P.S. and A.W.) with additional support (to A.W.) from the MRC and from HEFCE, Magnox and Varian Inc. for support toward instrumentation.

* To whom correspondence should be addressed. (P.S.) Phone: +44-(0)1865 275270; fax: +44-(0)1865 227259; e-mail: paul.spooner@bioch.ox.ac.uk. (A.W.) Phone: +44-(0)1865 275268, fax: +44-(0)1865 275234, e-mail: awatts@bioch.ox.ac.uk

[‡] University of Oxford.

[§] These authors contributed equally to the work.

^{||} Current Address: Department of Biochemistry, Max-Planck-Institute for Terrestrial Microbiology, 35043 Marburg, Germany.

[§] Leiden Institute of Chemistry.

^{||} University of Nijmegen Medical School.

¹ Abbreviations: GPCRs, G protein-coupled receptors; MAS, magic-angle spinning; ω_r , MAS sample rotation speed; $\Delta\omega_{iso}$, isotropic chemical shift frequency difference; T_2 , transverse relaxation time constant; T_2^* , zero-quantum relaxation time constant.

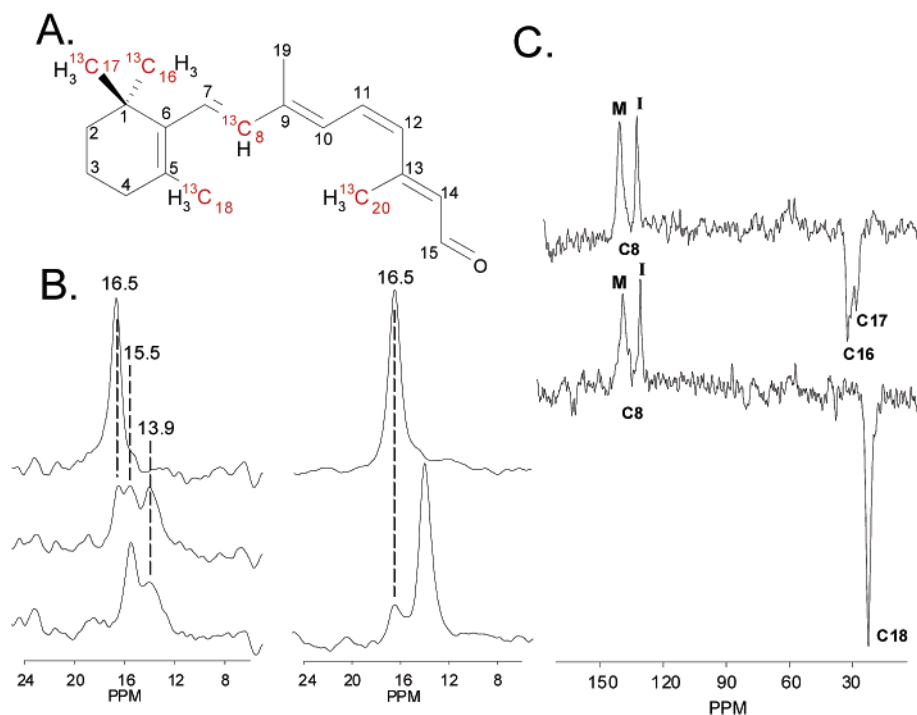


FIGURE 1: (A) Location of all ^{13}C -enriched nuclei (highlighted) in 11-*Z*-retinal used to regenerate rhodopsin in this study. Individually, the retinals were doubly labeled at two positions (C8 with either C18 or C16 and C17 in equal proportions). C20 was labeled with C10, but observations on C10 are not included here. (B) ^{13}C -background subtracted ^{13}C CP MAS NMR spectra from the C20 of [10, 20- $^{13}\text{C}_2$ -retinylidene]rhodopsin in the ground state (upper spectra) and following illumination at -30°C with light at $>570\text{ nm}$ for 10 min (middle, left) and 420 min (bottom, left), or after illumination with unfiltered white light at -196°C followed by warming to -20°C for 10 min (bottom right). (C) Background subtracted spectra obtained from the photoconverted samples of [8,16/17- $^{13}\text{C}_2$ -retinylidene]rhodopsin (top) and [8, 18- $^{13}\text{C}_2$ -retinylidene]rhodopsin (bottom). The C8 intensity is split into a narrow isorhodopsin component (I) and broad metarhodopsin-I component (M). Resonance M contains a contribution from residual rhodopsin remaining in the ground state ($\sim 18\%$) and the methyl group resonances have been inverted to prepare for rotational resonance exchange.

activity compared with metarhodopsin-II (7), the chromophore is expected to play a major role in triggering the activated state. Recent studies (8, 9) have revealed that the removal of the C19 methyl group (attached to C9, Figure 1A) from the chromophore results in a dramatic shift in the equilibrium from metarhodopsin-II to the inactive precursor, metarhodopsin-I, leading to the C19 methyl group being described as the “strongest factor” that influences transition to metarhodopsin-II (9). Modifications in and around the β -ionone ring that introduce greater flexibility within this segment were also shown to impair metarhodopsin-II formation, indicating that both the ring and the C19 methyl group of the chromophore make important steric contributions to protein activation (10). However, the direct importance of these interactions within the binding pocket on protein activation has been compromised by evidence obtained from photocrosslinking studies that the β -ionone ring of the chromophore is ejected from the binding pocket prior to formation of metarhodopsin-I (11, 12). For photolabeling, rhodopsin was regenerated with the ring-modified 3-diazo-4-keto-11-*Z*-retinal and then photointermediates were thermally trapped for photocrosslinking from C3 of the ring to track its movement within the protein. The ring was found to cross-link only with Trp²⁶⁵ within the binding pocket of the protein both in its resting and primary photointermediate (bathorhodopsin) states. However, at lumirhodopsin and the later intermediates, cross-linking was only observed with Ala¹⁶⁹ in helix-4, remote from the chromophore binding pocket. This suggests a remarkable conformational change at the early lumirhodopsin stage, disrupting major contacts

within the binding pocket and then no major adjustment in the location of the attached chromophore on progression to metarhodopsin-I and II. Taking this result at face value, and without evidence to the contrary, it is difficult to implicate the chromophore in any concerted conformational or electronic transformation leading to activation, other than to assume that these events are initiated on releasing the β -ionone ring from the binding pocket (13, 14). Another surprising feature of this study is that the modified chromophore seemed to drive the early photoequilibrium toward bathorhodopsin, since at the lumirhodopsin and later stages no cross-linking within any remaining ground-state rhodopsin was detected. Recent molecular dynamics calculations (15) predicted that the ring modified for photoaffinity cross-linking can induce deformations in the protein once flipped from its binding pocket, but did not consider whether modifications interfere with stabilizing interactions within the binding pocket.

The aim of the current study is to use high-resolution solid-state NMR methods to monitor changes in the conformation and environment around the ring segment of the chromophore on photoactivation of rhodopsin to the metarhodopsin-I stage. The strength of this approach is that rhodopsin is regenerated with the native chromophore enriched with nonperturbing ^{13}C nuclei, and that NMR observation is conducted *in situ*. Previously (16), we have used the rotational resonance solid-state NMR method to measure distances between the chain at C8 and each methyl group on the β -ionone ring (C16, C17, and C18) and showed that the chromophore adopts a 6-*s-cis* conformation in the ground

state and predicted a modest twist between the chain and the ring (C5–C6–C7–C8 torsion angle = $-28^\circ \pm 7^\circ$). This contradicted an earlier report from this laboratory (Oxford) that a twisted 6-s-trans conformation in the ground state was the most likely conformation for the ring, as deduced from NMR-derived orientations of methyl groups along the whole chromophore, and then modeled with available conformational information on the polyene chain (17). In comparison, the rotational resonance study was unambiguous in that it measured directly the conformation between the chain and the ring without any additional assumptions on conformation between these segments. The high-resolution features of ^{13}C NMR are particularly suitable for the current study in that the individual components of the photoequilibrium mixtures can be identified in the spectra and so can be examined separately. Combined with the frequency selectivity afforded by the rotational resonance method, distance measurements can in principle be performed for individual spectral components with little ambiguity. Observations here on ^{13}C at different locations in the polyene chain enable resolution and quantitation of all components in the photoactivated samples. Strong spectral broadening within the metarhodopsin-I component places unusual demands on the rotational resonance approach. However, these effects are compensated for by adaptations made in methodology and data treatment to achieve an effective comparison with the chromophore in the ground state.

EXPERIMENTAL PROCEDURES

Sample Preparation. The complete synthesis and purification of all doubly ^{13}C labeled retinals used in this study (shown together in Figure 1A) was as described previously (18). Bovine rhodopsin samples containing doubly labeled retinylidene, ([8,18- $^{13}\text{C}_2$] and [8,16/17- $^{13}\text{C}_2$]) were the same as used previously for rotational resonance analysis of the chromophore in its ground state (16). Additional rhodopsin samples in purified native membranes were obtained by regeneration with either 11-Z-[10,20- $^{13}\text{C}_2$]retinal or 11-Z-[16,17- $^{13}\text{C}_2$]retinal as described previously (16), except that the labeled compounds were used at a molar excess of 2:1 with respect to the protein, as compared to the equimolar amounts available for the previous study. Quantitative regeneration of the protein together with effective removal of excess retinal by washing with β -cyclodextrin, was confirmed in all membrane samples by UV spectroscopic analysis, as described (19). Protein was also regenerated with nonlabeled 11-Z-retinal to prepare the representative control membranes required for background subtractions in the ^{13}C NMR analysis. Membrane samples comprising between 7 and 15 mg of rhodopsin were loaded into 4-mm diameter MAS rotors and rotated briefly at moderate speed (few kHz) before freezing in liquid nitrogen for storage or measurement at -80°C . All manipulations prior to and following photoactivation were conducted in dim red light.

Photoactivation. The membranes with protein containing the labeled chromophore were photoactivated within the MAS rotors by first opening both ends of the rotor to expose the packed membrane. Membranes had packed as an annulus around the inside of the rotors so that the sample was also exposed along its entire length via a narrow central space. The open rotors were inserted into a close fitting hole bored

into the center of a copper cooling block whose temperature was controlled by immersion in a bath of various salt solutions with dry ice or in liquid nitrogen, allowing a range of individual temperatures to be maintained between -195 and -30°C ($\pm 1^\circ\text{C}$) and measured using a thermocouple inserted close to the sample position. Samples were irradiated from a 250W halogen Schott (Doncastor, UK) 2500 LCD source through two 5-mm diameter light guides that were fitted directly into the cooling block and flush with both ends of the open sample rotor. The light source was fitted with an infrared filter and an optional range of visible light filters. Following irradiation, the sample rotors could be warmed to higher temperature while in the block or transferred immediately to dry ice for reinserting the end plugs for NMR analysis. Rinsing of membrane samples with β -cyclodextrin solution to remove nonincorporated retinals also extracted a portion of the membrane lipid. Although the protein remains fully solvated in these membranes (> 30 lipids per protein) its normal transition from metarhodopsin-I to metarhodopsin-II is impaired following photoactivation (19). Despite this, the normal temperature range (-50 to -23°C) for trapping the metarhodopsin-I state was employed in the photoactivation methods. The metarhodopsin-I generated in this way had identical spectral characteristics (UV/Visible and FTIR, not shown) to that in the native membranes with full lipid complement.

NMR Methods. Membrane samples were analyzed at -80°C with a Chemagnetics (Varian Inc.) Apex MAS probe for 4-mm sample rotors and operating at 125.8 MHz for ^{13}C (500.1 MHz for protons) using CMX Infinity (Varian Inc.) spectrometer. Simple CP MAS observations were conducted at $\omega_r = 10.0$ kHz using a 20–30% linear ramp in radio-frequency amplitude around the Hartmann–Hahn condition for ^{13}C contact with a proton field strength of around 65 kHz. Rotational resonance exchange was measured only at the $n = 1$ condition ($\omega_r = \Delta\omega_{\text{iso}}$) using the standard procedure described previously (16) or by using a “constant time” version of this experiment (20) that required ^{13}C -background measurement from the nonlabeled membranes at only one exchange-time (usually 20 ms), and used extensive phase cycling throughout to minimize artifacts in the recorded signal. In both methods, the ramped-CP was used to create initial carbon magnetization that was manipulated subsequently with carbon pulses at field strength of 50 kHz. A proton decoupling field of 100 kHz was used during rotational resonance exchange and was attenuated to around 85 kHz for decoupling during signal acquisition. The fitting of on-resonance exchange curves was accomplished as described (16) and using relaxation times and tensor values as recorded previously (16). Exchange curves were compensated for inhomogeneous line broadening by generating a series of off-resonance exchange curves using a version of the original rotational resonance simulation program obtained from Malcolm Levitt (Southampton) and adapted by Clemens Glaubitz (Frankfurt). Exchange curves obtained by stepping away from the on-resonance condition at 20 Hz increments to cover a range of four times the line width, were combined using a Lorentzian weighting factor that incorporated the inhomogeneous line width, within the MATLAB (The MathWorks) software environment. This follows the approach introduced previously to include the effects of inhomogeneous broadening on rotational resonance

exchange rates (21). All chemical shifts are referenced to adamantane methylene (38.6 ppm).

RESULTS AND DISCUSSION

Photoactivation Conditions from Observations on the Chain-labeled Chromophore. Illumination of rhodopsin generates a mixture of photointermediate and photoregenerated states, and thus a detailed study was conducted to optimize conversion to the metarhodopsin-I photointermediate by varying conditions of illumination and temperature. These studies will be reported fully elsewhere but are summarized here to justify the conditions adopted for photoactivation of the rotational resonance samples. In previous NMR studies, it had been reported that around 50% of rhodopsin can be converted to the metarhodopsin-I state by first generating the primary photointermediate bathorhodopsin from illumination at liquid nitrogen temperature with white or blue light (22). Bathorhodopsin will then convert quantitatively to metarhodopsin-I at raised temperatures (> -50 °C). However, preliminary UV spectroscopic observations on dilute suspensions of regenerated membranes in these laboratories indicated that a higher conversion to metarhodopsin-I ($> 70\%$) could be achieved by generating this state directly at the elevated temperatures. For this, suspensions were illuminated with light at longer wavelengths (> 570 nm) that are preferentially absorbed by protein in its dark state compared with alternative intermediate or regenerated photoproducts. This direct photoactivation to the metarhodopsin-I intermediate was examined in the NMR samples from protein regenerated with ^{13}C at C10 and C20, around the position of photoisomerization in the polyene chain of the chromophore. The resolution between photoproducts and unconverted protein was best for the C20 methyl group and only spectra for this labeled position are shown here. The chemical shift of 16.5 ppm recorded for C20 in ground-state rhodopsin (Figure 1B, upper spectra) is close to that observed (23) in the detergent-solubilized protein (16.8 ppm, as quoted in ref 24). Changes in the C20 resonance during illumination of the NMR sample at -30 °C with light of wavelength > 570 nm (Figure 1B, stacked to left) show the emergence of a component at low ppm (13.9) where metarhodopsin-I is expected to appear (24), along with an additional component at 15.5 ppm (middle spectrum) that grows with increasing irradiation time at the expense of intensity at the metarhodopsin-I shift (bottom spectrum). This component is assigned to [7-Z-retinylidene]rhodopsin, which can form slowly by photoreisomerization of the all-trans chromophore in lumirhodopsin and metarhodopsin-I (25), but accumulates to high levels here due to its lack of absorption and subsequent re-conversion under light at longer wavelengths. In the time required to convert rhodopsin in these NMR samples (~ 70 min; data not shown), significant amounts of bathorhodopsin were converted into [7-Z-retinylidene]rhodopsin and possibly also [9-Z-retinylidene]rhodopsin (isorhodopsin). The isorhodopsin component was not resolved from metarhodopsin-I in the C20 spectra and is assigned the same chemical shift (13.9 ppm). Attempts to suppress photoconversion of metarhodopsin-I to [7-Z-retinylidene]rhodopsin by using longer wavelength light for excitation (> 610 nm) were unsuccessful, due to the very slow conversion of ground-state rhodopsin under these conditions. Hence, the direct method of metarhodop-

sin-I generation was not used for the experimental rotational resonance samples.

To avoid generating additional ground-state products through photoconversion of metarhodopsin-I, this photointermediate was produced "indirectly" from the primary photoproduct, bathorhodopsin, generated at temperatures close to liquid nitrogen (-188 to -190 °C). Here, the shorter wavelengths (430–460 nm) should be optimal for illumination since these are preferentially absorbed by the unwanted participants in this photoequilibrium, namely, rhodopsin in the ground state and isorhodopsin. These short wavelengths were found to provide a very low photoconversion of ground state rhodopsin in the NMR samples with the experimental setup used here, over lengthy periods of illumination (up to 600 min). Given that weaker illumination at 460 nm had previously been successful for thin layers of purified and solubilized protein in NMR rotors (22), it is concluded that the shorter wavelength light penetrated poorly the dense membrane preparations used in the work reported here. The "indirect" conversion was therefore conducted with unfiltered white light for a period that shows effective conversion of rhodopsin according to the spectrum from the C20 resonance, as shown in Figure 2B (stacked to right). This sample was warmed to -20 °C (10 min) to convert the primary intermediate to the metarhodopsin-I form prior to measurement. The residual intensity in the C20 spectra showed that less than 20% of the rhodopsin remained in the ground state following this procedure (17 and 19% in two separate samples). This conversion level is somewhat better than reported for steady state mixtures obtained from short wavelength illumination (25–30% remaining as rhodopsin; ref 22). The photoproducts now appear as a single resonance (13.9 ppm) in the C20 spectrum, but this again includes some isorhodopsin that is not resolved from C20 in metarhodopsin-I. Although the observations on C20 in the test samples with [10, 20- $^{13}\text{C}_2$ -retinylidene]rhodopsin show good conversion of ground state protein by these illumination procedures, the resultant levels of the desired metarhodopsin-I could only be finally deduced from the rotational resonance samples which provide optimal resolution for isorhodopsin in the C8 resonance (22), as described below.

Photoconversion of the Rotational Resonance Samples. Photoactivation by the indirect procedure described above, on samples containing ^{13}C at either C8 and C18 or at C8 with C16 and C17 in equal proportions only produced large changes in the C8 region of the spectra as shown in the background-subtracted spectra in Figure 1C. The C8 intensity in both samples splits into a narrow component at 131.1 ppm (~ 120 Hz line width), corresponding to the chemical shift reported previously for C8 in isorhodopsin (22), and a very broad component at 139.4 ppm comprising some residual rhodopsin, but mainly the photoproduct, metarhodopsin-I. Since the chemical shift is unchanged in this C8 component from that in ground-state rhodopsin (16), the large chemical shift dispersion in this line (> 400 Hz line width) is attributed to structural inhomogeneity existing around C8 in the chain of metarhodopsin-I.

The only significant chemical shift change that could be detected for the ring methyl groups on photoactivation was in the C18 resonance, which increased from 22.1 to 22.5 ppm. The large splitting between C16 and C17 (-4.3 ppm) describes the unique orientation of these geminal methyl

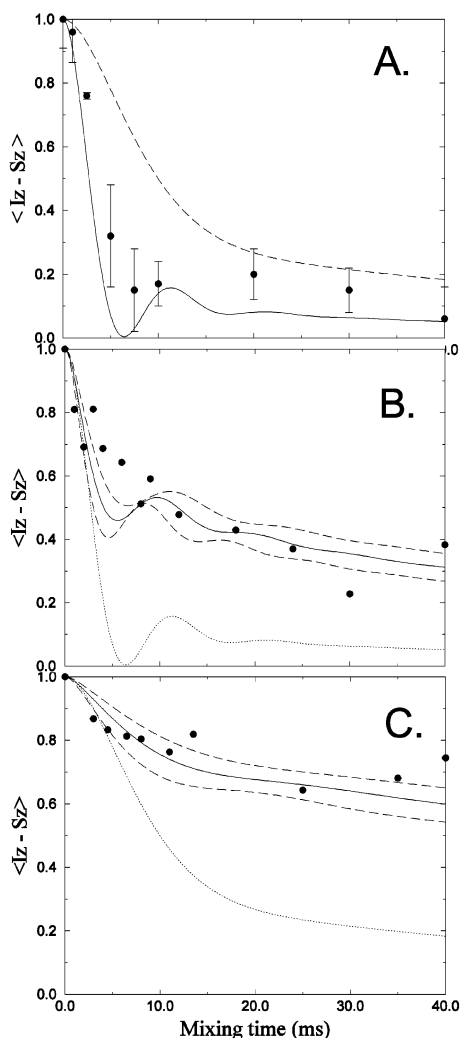


FIGURE 2: (A) Exchange data under $n = 1$ rotational resonance between C8 and C18 in isorhodopsin. The net magnetization $\langle I_z - S_z \rangle$ was corrected for the proportion of C18 (39%) that existed in the isorhodopsin form, and is displayed as a function of rotational resonance mixing time. Magnetization exchange curves were those fitted previously (16) to exchange between C8 and C18 (at 2.95 Å separation: lower, solid line) and between C8 and both C16 and C17 (at 4.05 Å separation: upper broken line) in ground-state rhodopsin and represent exchange rates expected for a 6-s-cis or planar 6-s-trans conformation, respectively. (B, C) Exchange data under $n = 1$ rotational resonance between C8 and C18 (B) or C17 (C) in metarhodopsin-I using the constant time method. The lower curves (dotted) in each case were those fitted to the corresponding exchange data measured in the ground-state protein and then after including the effects of inhomogeneous broadening for the C8 resonance in metarhodopsin-I (solid lines) together with corrected curves representing the upper and lower limits (upper and lower dashed curves, respectively) of the distances from the chromophore in the ground-state protein (4.05 ± 0.25 Å between C8 and C17 in B; 2.95 ± 0.15 Å between C8 and C18 in C).

groups in rhodopsin (16), and its retention on photoactivation is important for the structural arguments presented in the following discussion. An overall increase in line width with no significant alteration in chemical shift for the conformationally sensitive C8 resonance, suggests that in metarhodopsin-I, this segment of the chain in the chromophore varies in conformation around its original structure found in the ground state of the protein, leading to a larger range of intramolecular steric interactions. The narrower C8 resonance from isorhodopsin comprised 39% of the C8 intensity from

the sample with C18 and 37% of the C8 intensity from the sample with C16 and C17 labels. These isorhodopsin levels are higher than estimated from the steady state mixture with bathorhodopsin (~25%), as previously analyzed by NMR (22), probably due to the necessity of using unfiltered white light rather than blue light for effective photoactivation in the membrane samples studied here. Nonetheless, the resultant lower levels of ground-state rhodopsin (~18%) in the samples are preferred for detecting any overall change in conformation on photoactivation by the rotational resonance method, since this component is not resolved from the C8 in metarhodopsin-I and thus will contribute less to the exchange observed with the ring methyl group signals in these samples. Since the C8 for isorhodopsin is well resolved and will not participate in rotational resonance exchange in metarhodopsin-I, its impact is restricted to reducing the proportion of exchanging intensity in these experiments. This effect is not trivial, however, since it makes the quantitation of exchange technically more demanding for the C8 resonance in metarhodopsin-I, for which signal-to-noise is already limited by strong line broadening, and for the ring methyl signals that are composites of all forms in the photoactivated mixtures. As noted previously (16), the C8 chemical shift is highly sensitive to the isomeric state around the C6–C7 bond between the ring and the chain. In metarhodopsin-I, the C8 chemical shift is unchanged from the ground state of the protein and remains well within the shift range expected for 6-s-cis forms but C8 for isorhodopsin falls within the chemical shift range expected from the alternative 6-s-trans configuration (16).

The Conformation in Isorhodopsin and Metarhodopsin-I. The standard rotational resonance experiment (Experimental Procedures) was used to observe the exchange between C8 in isorhodopsin and C18 in the ring and the net magnetization ($\langle I_z - S_z \rangle$), corrected for the proportion of participating signal, is shown as a function of rotational resonance mixing time in Figure 2A. The relatively large error bars on the exchange data reflect uncertainties in quantitation of peak intensities where signal-to-noise and the number of experimental points is limited by the length of time required to complete the standard rotational resonance experiment. Nevertheless, the exchange behavior is shown to follow quite closely the lower curve that was fitted to the rapid exchange observed previously between C8 and C18 in ground-state rhodopsin (16), indicating that the C8–C18 distance remains close (~3 Å) in isorhodopsin and that this isomer therefore retains the preferred 6-s-cis conformation in the protein binding pocket. The upper curve shown in Figure 2A was fitted previously to the combined data for exchange between C8 and both C16 and C17 and is used here to show that the initial exchange in isorhodopsin is significantly faster than expected over the fitted C8, C16/17 distance (4.05 Å), which approximates that between C8 and C18 in a planar 6-s-trans conformer. The large steric shift to lower ppm observed for C8 in isorhodopsin evidently does not arise from interaction with the ring methyl groups as in the case of the 6-trans forms of retinal analogues, but from the 9-Z configuration creating close interactions within the chain (e.g., between the C8 and the C11 proton).

On the basis of the measurements made on photoactivated [10, 20-¹³C₂-retinylidene]rhodopsin, the broad nonshifted C8 spectral component includes a contribution of around 18%

from rhodopsin that remains in the ground state. Including the measurements on isorhodopsin, the overall levels of metarhodopsin-I were estimated to be 43 and 45% in the photoactivated mixtures obtained from the [8,18- $^{13}\text{C}_2$ -retinylidene] and [8,16/17- $^{13}\text{C}_2$ -retinylidene]rhodopsin samples, respectively. The demands of reliably quantifying exchange between a portion of the spectral intensity from ring methyl groups and the broad C8 resonance in metarhodopsin-I could not be met by the standard protocol for rotational resonance. Instead, data of acceptable quality could be recorded for a limited number of rotational resonance mixing times using the shorter and more robust "constant time" (see Experimental Procedures) version of this experiment that minimized the effects of various instrumental instabilities (20). The rotational resonance data obtained by this method for exchange between the ring methyls and the broad C8 resonance, representing mostly metarhodopsin-I, are shown in Figure 2B,C. Of the methyl pair at C1, only the exchange with the lower chemical shift component assigned to C17 is included (see Figure 1C) since some broadening in these methyl group resonances (50–70 Hz) made reliable deconvolution of C16 from the close minor components, as identified previously in this sample (16) too difficult to perform.

The exchange rates observed in both samples are strongly damped compared with that observed in the ground-state of the protein, as illustrated by the exchange curves that had been fitted to the previous data (16) prior to photoactivation (dotted lines in Figure 2B,C). All the exchange data have been corrected for the proportion of ring methyl spectral intensity participating in the metarhodopsin-I rotational resonance exchange, but still include the contribution from nonresolved rhodopsin remaining in the ground state (~18%). The reliability in the experimental data was no longer dictated by uncertainties in the peak quantitation, the constant time data being obtained with better signal-to-noise over a reasonable time and with more reproducible spectral subtraction, and so error bars for quantitation of spectral intensity were not included. Variability in these measurements should be largely determined by instrumental instabilities that are difficult to assess but are minimized by application of the "constant-time" method. The exchange rates corresponding to the inter-nuclear distances and their estimated limits determined for the ground state (2.95 ± 0.15 Å between C8 and C18; 4.05 ± 0.25 Å between C8 and C17) were then corrected for resonance offset effects due to inhomogeneous broadening of the C8 in metarhodopsin-I according to the procedure given in Experimental Procedures. For this, a full C8 line width of 410 Hz was first corrected for a homogeneous contribution of 31 Hz, obtained from a T_2 of 10.3 ms for C8, giving an inhomogeneous line width of 379 Hz. Exchange curves were then calculated using this line width with the original distances for the ground-state protein and a T_2^{ZQ} of 6 ms, as estimated from the combined T_2 values and used as a starting value in the previous analyses (16).

The compensated exchange curves are given in Figure 2B,C and show that the internuclear distances and their limits (solid and dashed curves, respectively) recorded from the ground-state rhodopsin also represent reasonably well the exchange behavior observed in metarhodopsin-I. It is possible that the early exchange behavior (5–10 ms) including the

distinct oscillatory feature for the short distance between C8 and C18 cannot be well reproduced due to structural inhomogeneity that is apparent in this chain segment of metarhodopsin-I from the chemical shift dispersion in the spectra. Despite the structure being less well defined in the current observations, the exchange behavior indicates that the average conformation between the ring and adjoining chain segment of the chromophore is largely retained on conversion of rhodopsin to the metarhodopsin-I state.

In the previous modeling of the chromophore in its ground-state (16), the torsion angle defining the twist between the ring and the chain is negative and quite modest (C5–C6–C7–C8 torsion angle -28°) and C8 is equidistant between the ring methyl groups at C1 with C17 turned into *axial* orientation, in agreement with rotational resonance and chemical shift data. It has been predicted (26) that on relaxation from bathorhodopsin, C8 must move past the C18 methyl group thereby reversing the sense of rotation between the ring and the chain. Despite not being able to measure exchange to both methyl groups at C1, we currently conclude from the data for C17 alone that the chain of the chromophore in metarhodopsin-I also retains the same sense of rotation around the C6–C7 bond as in the ground state protein. This is based on the observation that the asymmetric orientation of C16 and C17 about the ring plane remains unchanged in metarhodopsin-I. A reversal in the sense of twist in the chain (positive torsion) would significantly lengthen the distance between C8 and C17 since all positive torsion angles place C8 at least 4.5 Å from C17, restricting exchange to above the upper dashed limit curve in Figure 2B (4.3 Å).

Location of the Chromophore in Metarhodopsin-I. The lack of change in the characteristic spectral splitting between the C16 and C17 methyl groups on photoactivation is central to our overall conclusion that the entire chromophore is retained within the binding pocket of the protein. This result was confirmed with a further sample of rhodopsin that was regenerated in native membranes with the chromophore ^{13}C -labeled at >99% in both C16 and C17, rather than being distributed between these methyl groups in equal proportions (~50%), as present in the rotational resonance sample with C8. This samples showed better resolution between the C16 and C17 resonances due to the absence of minor forms, as observed in the rotational resonance samples, and again showed no significant change in chemical shift for these components (within 0.1 ppm) on photoactivation to the metarhodopsin-I state (data not shown). As identified previously (16), this splitting arises from a classical γ -effect from the C17 methyl group being tilted out of the ring plane into *axial* orientation and interacting sterically with the proton on C3 of the ring (H3 in Figure 3A). The magnitude of the steric shift on the C17 resonance (-4.3 ppm) was the largest observed for this ring system and is therefore considered diagnostic of the β -ionone ring being restrained with its strong contacts within the binding pocket. The conviction that the ring remains unperturbed within the binding pocket up to metarhodopsin-I also relies on the sensitivity of the C17 chemical shift to any conformational relaxation. So far the C17 chemical shift has remained reproducible within 0.1 ppm following photoactivation, although experimental variability of ± 0.1 ppm would not be unexpected from errors in subtracting background contributions from the spectra.

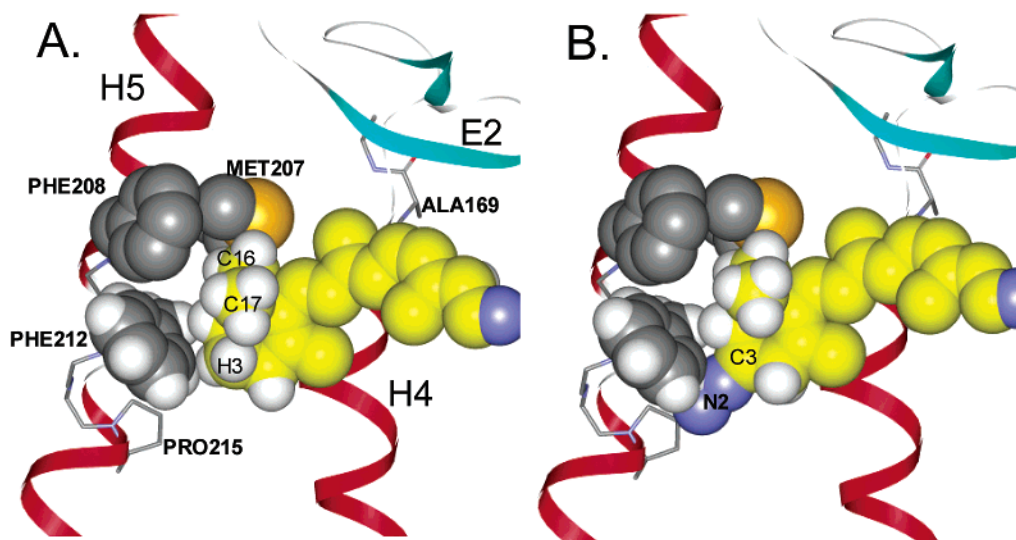


FIGURE 3: Binding pocket contacts for the chromophore ring with residues on helix-5 (H5) of rhodopsin. The binding pocket is derived from the latest crystallographic structure of the rhodopsin in the ground state (28) and the chromophore in A (shown in yellow) was modeled with NMR restraints for the ring segment obtained previously (16) using Insight II (Accelrys Inc.) and aligned with the ring location provided in the crystallographic structure (DS Viewer Pro, Accelrys Inc.). The binding pocket is viewed perpendicular to the membrane normal (and to the face of the chromophore ring) and with the extra-cellular side of the protein above. Phe²¹² appears within a flexible region of helix-5 (H5) above Pro²¹⁵ and contacts the C2–C3 edge of the ring. Ala¹⁶⁹, the site of photolabeling in the early photointermediate, lumirhodopsin, is shown behind the chromophore (and the inter-helical loop E2), is situated at the top of the short helix-4 (H4) and is around 15 Å from C3 on the ring. The primary restraints to the ring rotating out of the binding pocket toward Ala196 are from Met²⁰⁷ and Phe²⁰⁸. In B, the chromophore ring is shown in the same location within the binding pocket but has been modified with a diazo group (N2) attached to C3 as in the photocrosslinking analogue. The diazo group cannot be accommodated in this position since it penetrates through the van de Waal space at the bottom of Phe²¹². This structural modification of the ring required that the C2–C3–C4 segment be made approximately coplanar with the C3–N2 bond (Insight II) to reflect the changes in hybridization at C3 and also C4 (keto group not shown) in the photoaffinity analogue.

According to semiempirical calculations (27) of the steric shift applied to our ground-state model of the chromophore (16), a 0.2 ppm decrease in the shift would result from C17 being allowed to move just 0.02 Å (2 pm) back toward the ring plane or a change of 0.5° in the tilt of the C17 methyl group (C4–C5–C6–C17 torsion angle). Therefore, the current observations clearly do allow for any significant disruption of the contacts around C16 and C17 on the ring and furthermore make it unreasonable that such contacts could be reproduced at any alternate location within the protein. The only remaining concern could be that, although according to UV/Visible and FT-IR analysis the photointermediate studied here is spectrally identical to metarhodopsin-I in native membranes, the reduced lipid in our systems has resisted some subtle conformational change that can release the chromophore ring. Partly to investigate this possibility, we have recently observed C16 and C17 in rhodopsin that was isolated from lipid-reduced membranes and reconstituted with native lipids at the full complement found in native membranes (60 lipids per protein) and again note no significant change in the chemical shifts of these groups on progression to metarhodopsin-I (data not shown).

Reevaluation of the Photocrosslinking Studies. The overall conclusion of this work is that the ring of the chromophore is retained in its original location in the protein up to metarhodopsin-I, which is in stark contrast to the previous evidence from photocrosslinking experiments that the ring flips out of the binding pocket at lumirhodopsin, prior to metarhodopsin-I and extends across the helical bundle to interact with helix-4 (at Ala¹⁶⁹). The primary contacts resisting such motion, based on the ground-state crystallographic structure of the protein (28) are shown in Figure

3A to involve residues on helix-5: Phe²⁰⁸ and particularly Met²⁰⁷ which is in contact with the C16 methyl group on the ring. There is no evidence for any major structural reorganization around the native environment of the binding site prior to activation of the protein although a recent report has predicted a counterion switch, with possible structural changes around the Schiff base end of the chain (29, 30). The C2–C3 edge of the ring is abutted with Phe²¹² on helix-5 and so this configuration and the associated contacts for the ring would be expected to be especially sensitive to modifications along this ring border. As shown in Figure 3B, with the ring in its original location, the photoreactive diazo group introduced onto C3 for the photocrosslinking experiments could not be accommodated since it penetrates through the van de Waal space at the base of Phe²¹². The analogue must therefore either reposition the ring within the binding pocket or alternatively displace the contacting residues on helix-5. The latter option would seem more likely following photoactivation as the chromophore seeks to release the strain of isomerization within the chain. This is also favored by the contacting residues on helix-5 being situated close to Pro²¹⁵, which does not strongly distort helix-5 in the ground state structure but appears to create a flexible region in the backbone especially at Phe²¹². On the basis of these insights from the protein structure and the results presented here, we propose that steric violations displace the ring of the photoaffinity analogue in the ground-state protein to enable the reported cross-linking with Trp²⁶⁵ (11) which overlaps the C18 methyl group on the native ring structure. Then following photoisomerisation, steric clash with the ring could force helix-5 to kink at Phe²¹² thus carrying away the primary restraining residues and open a

channel for the rotational flip and translation of the ring toward Ala¹⁶⁹ on helix-4.

ACKNOWLEDGMENT

The authors thank Lynmarie Thompson (University of Massachusetts, Amherst) for providing a pulse program that was adapted in the current work for constant time rotational resonance.

REFERENCES

1. Palczewski, K., Kumasaka, T., Hori, T., Behnke, C. A., Motoshima, H., Fox, B. A., Le Trong, I., Teller, D. C., Okada, T., Stenkamp, R. E., Yamamoto, M., and Miyano, M. (2000) *Science* 289, 739–745.
2. Teller, D. C., Okada, T., Behnke, C. A., Palczewski, K., and Stenkamp, R. E. (2001) *Biochemistry* 40, 7761–7772.
3. Ballesteros, J. A., Jensen, A. D., Liapakis, G., Rasmussen, S. G. F., Shi, L., Gether, U., and Javitch, J. A. (2001) *J. Biol. Chem.* 276, 29171–29177.
4. Lu, Z.-L., Saldanha, J. W., and Hulme, E. C. (2002) *Trends Pharm. Sci.* 23, 140–146.
5. Mirzadegan, T., Benko, G., Filipek, S., and Palczewski, K. (2003) *Biochemistry* 42, 2759–2767.
6. DeGrip, W. J., and Rothschild, K. J. (2000) in *Handbook of Biological Physics, Vol. 3, Molecular Mechanisms of Visual Transduction* (Stavenga, D. G., DeGrip, W. J., Pugh, E. N., Jr., Eds.) Ch. 1, pp 1–54, Elsevier, Amsterdam.
7. Melia, T. J., Jr., Cowan, C. W., Angleson, J. K., and Wensel, T. G. (1997) *Biophys. J.* 73, 3182–3191.
8. Vogel, R., Fan, G.-B., Sheves, M., and Siebert, F. (2000) *Biochemistry* 39, 8895–8908.
9. Meyer, C. K., Böhme, M., Ockenfels, A., Gärtner, W., Hofmann, K. P., and Ernst, O. P. (2000) *J. Biol. Chem.* 275, 19713–19718.
10. Jäger, F., Jäger, S., Kräutle, O., Friedman, N., Sheves, M., Hofmann, K. P., and Siebert, F. (1994) *Biochemistry* 33, 7389–7397.
11. Borhan, B., Souto, M. L., Imai, H., Shichida, Y., and Nakanishi, K. (2000) *Science* 288, 2209–2212.
12. Souto, M. L., Um, J., Borhan, B., and Nakanishi, K. (2000) *Helv. Chim. Acta* 83, 2617–2628.
13. Jang, G.-F., Kuksa, V., Filipek, S., Bartl, F., Ritter, E., Gelb, M. H., Hofmann, K. P., and Palczewski, K. (2001) *J. Biol. Chem.* 276, 26148–26153.
14. Ernst, O. P., and Bartl, F. J. (2002) *ChemBioChem* 3, 968–974.
15. Ishiguro, M., Hirano, T. and Oyama, Y. (2003) *ChemBioChem* 4, 228–231.
16. Spooner, P. J. R., Sharples, J. M., Verhoeven, M. A., Lugtenburg, J., Glaubit, C., and Watts, A. (2002) *Biochemistry* 41, 7549–7555.
17. Gröbner, G., Burnett, I. J., Glaubit, C., Choi, G., Mason, A. J., and Watts, A. (2000) *Nature* 405, 810–813.
18. Groesbeek, M., and Lugtenburg, J. (1992) *Photochem. Photobiol.* 56, 903–908.
19. DeLange, F., Bovee-Geurts, P. H. H., VanOostrum, J., Portier, M. D., Verdegem, P. J. E., Lugtenburg, J., and DeGrip, W. J. (1998) *Biochemistry* 37, 1411–1420.
20. Balazs, Y. S., and Thompson, L. K. (1999) *J. Magn. Res.* 139, 371–376.
21. Heller, J., Larsen, R., Ernst, M., Kolbert, A. C., Baldwin, M., Prusiner, S. B., Wemmer, D. E., and Pines, A. (1996) *Chem. Phys. Lett.* 251, 223–229.
22. Smith, S. O., Courtin, J., De Groot, H., Gebhard, R., and Lugtenburg, J. (1991) *Biochemistry* 30, 7409–7415.
23. Smith, S. O., Palings, I., Miley, M. E., Courtin, J., DeGroot, H., Lugtenburg, J., Mathies, R. A., and Griffin, R. G. (1990) *Biochemistry* 29, 8158–8164.
24. Verdegem, P. J. E., Bovee-Geurts, P. H. M., DeGrip, W. J., Lugtenburg, J., and DeGroot, H. J. (1999). *Biochemistry* 38, 11316–11324.
25. Maeda, A., Ogurusu, T., Shichida, Y., Tokunaga, F., and Yoshizawa, T. (1978) *FEBS Lett.* 92, 77–80.
26. Lewis, J. W., Fan, G.-B., Sheves, M., Szundi, I, and Kliger, D, S. (2001) *J. Am. Chem. Soc.* 123, 10024–10029.
27. Grant, D. M., and Cheney, B. V. (1967) *J. Am. Chem. Soc.* 89, 5315–5318.
28. Okada, T., Fujiiyoshi, Y., Silow, M., Navarro, J., Landau, E. M., and Shichida, Y. (2002) *Proc. Natl. Acad. Sci. U.S.A.* 99, 5982–5987.
29. Yan, E. C. Y., Kazmi, M. A., Ganim, Z., Hou, J.-M., Pan, D., Chang, B. S. W., Sakmar, T. P., and Mathies, R. A. (2003) *Proc. Natl. Acad. Sci. U.S.A.* 100, 9262–9267.
30. Birge, R. R., and Knox, B. E. (2003) *Proc. Natl. Acad. Sci. U.S.A.* 100, 9105–9107.

BI0354029